metals

MDPI

Article

Synchronous Upgrading Iron and Phosphorus Removal from High Phosphorus Oolitic Hematite Ore by High Temperature Flash Reduction

Deqing Zhu, Zhengqi Guo *, Jian Pan * and Feng Zhang

School of Mineral Processing and Bioengineering, Central South University, Changsha 410083, China; dqzhu@csu.edu.cn (D.Z.); zhangfengcsu@126.com (F.Z.)

* Correspondence: gzqcsu@126.com (Z.G.); pjcsu@csu.edu.cn (J.P.); Tel.: +86-185-7313-1417 (Z.G.); +86-138-7314-2654 (J.P.); Fax: +86-731-8883-6942 (Z.G. & J.P.)

Academic Editor: Corby G. Anderson

Received: 31 March 2016; Accepted: 11 May 2016; Published: 24 May 2016

Abstract: In this paper, an effective method was developed to remove phosphorus and upgrade iron from high phosphorus oolitic hematite ore by high temperature flash reduction—a wet magnetic separation process. A thermodynamic analysis of iron and phosphorus mineral reactions and experiments with Fe-P separation process were performed, and the mechanism of phosphorus removal and beneficiation of iron is discussed as well. The results show that under the proper conditions, a final metallic iron powder assaying over 91% Fe and 0.25% P was obtained with iron recovery of 90% and phosphorus removal rate of 91.79% using the new process, indicating that the high temperature flash reduction process is a feasible and efficient way to process this kind of complex and refractory iron ore. Moreover, sodium sulfate is found to be capable of improving the removal of phosphorus and the upgrading of iron, as well as enhancing the growth of metallic iron grains significantly for higher recovery of iron.

Keywords: high temperature reduction; phosphorus removal; oolitic hematite ore; sodium sulfate

1. Introduction

Oolitic hematite ore, one type of the most refractory iron ores, is characterized by low total iron grade (Fe_{total} 35%–50%), high phosphorus and aluminum content (0.4%–1.8% P and 2.5%–9.0% Al_2O_3, respectively), as well as poor liberation of iron minerals due to fine dissemination [1,2]. However, the proven reserves of this type of iron ore are relatively abundant, reaching approximately 4.0 billion tons only in China. If oolitic hematite ore were properly processed with effective technologies, the increasing pressure of an iron resource shortage would be reduced.

In recent years, many efforts have been focused on improving the beneficiation of iron and the removal of phosphorus from oolitic hematite ore, such as chemical leaching [3–5], bio-leaching [6–8], magnetic roasting [9], selective agglomeration-reverse flotation [10], physical separation and direct reduction-magnetic separation [11,12]. Note that the direct reduction process to upgrade this type of complex and refractory iron ore has been a topic of metallurgical interest lately.

Ba *et al*. noted that an iron concentrate with 76.47% Fe and 0.25% P was obtained under following conditions: pelletizing the mixture of oolitic hematite ore with 10% Na_2CO_3, reducing the pellets at 1050 °C for 180 min and with C/Fe (mass ratio) of 0.82 [13].

Li *et al*. reported the effect of sodium sulfate on reduction roasting and P removal from high-phosphorus oolitic hematite ore. The results showed that a magnetic concentrate with total iron grade of 92.7% and phosphorus content of 0.09% was produced from an oolitic hematite ore containing 48.96% iron and 1.61% phosphorus, where reduction of the iron ore blended with excessive coal at 1050 °C for 120 min with 9.0% sodium sulfate was conducted. Moreover, the results also confirmed that sodium sulfate is favorable for improving the beneficiation of iron and the removal of phosphorus through reacting with the gangues and destroying the concentric and layered oolitic structure [14].

Li *et al*. extracted the iron from oolitic hematite ore by deep reduction at 1200 °C for 60 min with 25% coal content followed by wet-magnetic separation of the reduced ore, with the iron powder produced containing 91.35% Fe_{total}, 0.087% P with a corresponding iron recovery of 85.32% [15].

Indeed, this research on the direct reduction process is effective for simultaneous beneficiation of iron and removal of phosphorus. However, as traditional direct reduction processes, the amount of coal generally required is too much and the reduction duration is always very long, resulting in high energy consumption and low productive efficiency. Thus, an innovative technology for recovering iron and phosphorus removal from oolitic hematite ore is proposed in this paper: high temperature flash reduction-wet magnetic separation in the paper. In this new process, sodium sulfate was also employed to enhance the reduction roasting of oolitic hematite ore, growth of metallic iron grains and removal of phosphorus in a short time, thus improving the efficiency.

2. Experimental

2.1. Raw Materials

2.1.1. Oolitic Hematite Ore

The oolitic hematite ore with high phosphorus content used in the paper was collected from Western Hubei, China. The chemical composition of oolitic hematite raw ore is shown in Table 1. The main ingredients contained in the sample were 41.50 wt. % Fe and 17.04 wt. % SiO_2, while the content of phosphorus was as high as 1.24 wt. %.

Table 1. Chemical composition of oolitic hematite ore/wt. %.

TFe	P	SiO_2	Al_2O_3	CaO	MgO	K_2O	S	LOI *
41.50	1.24	17.04	4.68	7.82	1.54	0.9	0.09	5.72

* LOI—loss on ignition

The XRD spectrum of average sample is showed in Figure 1, which indicates that the main iron-bearing mineral in the oolitic hematite is hematite, and major gangue minerals include quartz, chlorite and apatite observed in the oolitic hematite. Chemical phases and distribution of phosphorus in oolitic hematite ore is listed in Table 2. It is noted that the phosphorus mainly occurs in apatite, which accounts for 94.76% of the total phosphorus.

Table 2. Chemical phases and distribution of phosphorus in oolitic hematite ore /wt. %.

Mineral	Apatite	Iron Phosphate	Others	Total Phosphorus
Content	1.175	0.041	0.024	1.24
Fraction	94.76	3.31	1.94	100

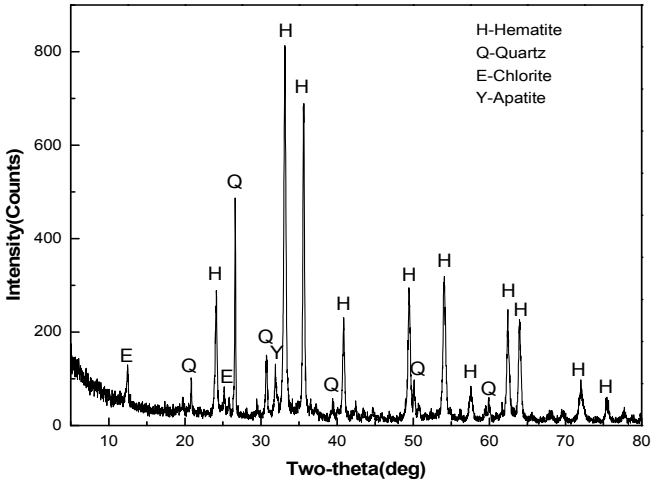

Figure 1. X-ray diffraction pattern of the oolitic hematite ore.

Figure 2 presents micrographs of oolitic hematite ore observed under optical microscopy and the scanning electron microscopy (SEM) image, and the results of energy dispersive spectroscopy (EDS) measured at different points of the hematite are shown in Figure 3. It is clear that the sample contains many ooids with concentric layers of alternate iron-bearing minerals and gangue minerals. In addition, the hematite, as the main iron-bearing mineral, occurs closely with chlorite and quartz forming concentric shell. Meanwhile, the hematite grain is finely disseminated with gangue minerals. Very often the phosphorus is present as apatite groups, which are embedded in gangue minerals, or even partly surrounded by ooids. Therefore, in light of extremely complex mineralogical structure of oolitic hematite ore, it is relatively difficult to beneficiate the iron and to remove phosphorus by traditional physical separation processes.

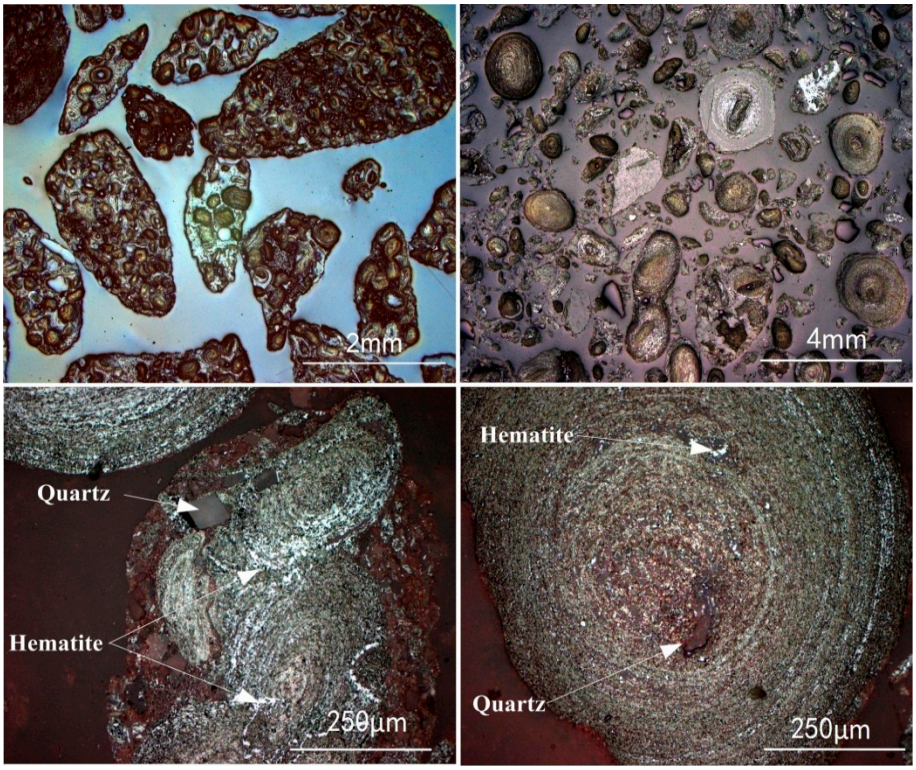

Figure 2. Optical microscope pictures of the oolitic hematite ore.

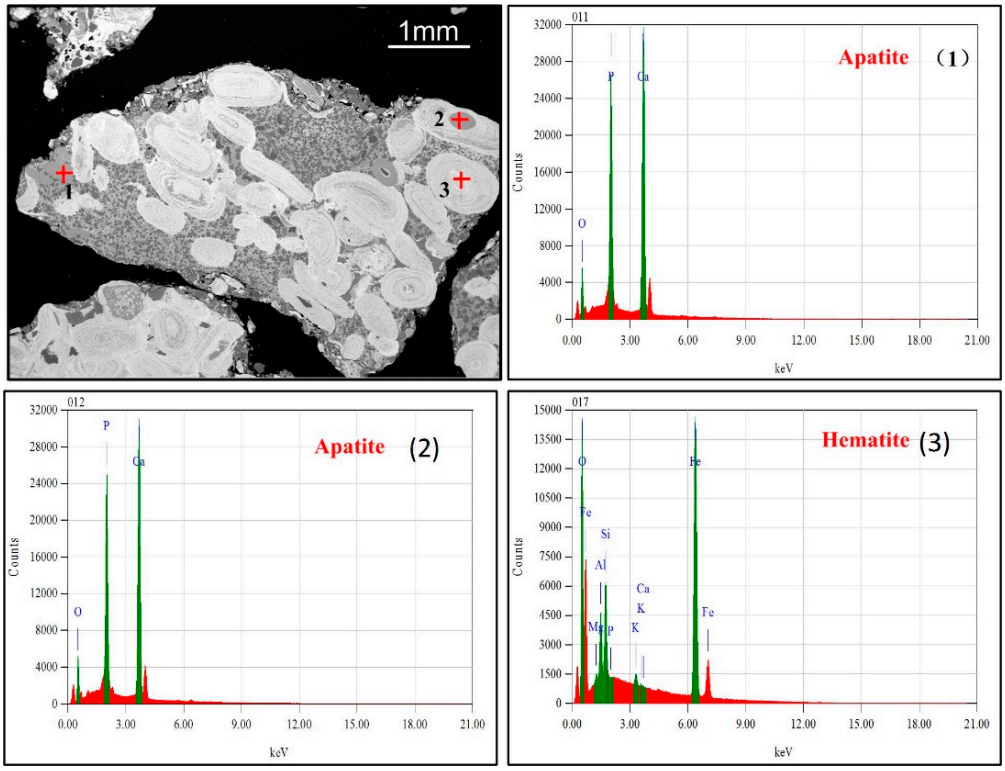

Figure 3. SEM images and EDS energy spectra of the oolitic hematite ore.

2.1.2. Reducing Coal

The soft coal was used as reducing agent. The main chemical composition of coal ash and the proximate and fusibility analysis of soft coal were determined by GB/T212-2008 and GB/T219-2008, respectively, and results are shown in Tables 3 and 4 respectively. It can be seen that the soft coal bears a low ash content of 4.49%, moderate fixed carbon content of 52.12% and appropriate volatiles content of 30.41%. It also possesses the proper ash fusibility, making it a superior reducing agent and suitable to be adopted in the research.

Table 3. Main chemical composition of coal ash/wt. %.

Fe_2O_3	SiO_2	Al_2O_3	CaO	MgO	P	S
16.70	27.62	8.02	24.94	1.34	0.01	5.17

Table 4. Proximate and fusibility analysis results of soft coal.

Proximate Analysis/%				Ash Fusibility Analysis/°C			
M_{ad}	A_{ad}	V_{ad}	FC_{ad}	DT	ST	HT	FT
12.98	4.49	30.41	52.12	1332	1376	1450	1469

M_{ad}: Mositure; A_{ad}: Ash; V_{ad}: Volatile Matter; FC_{ad}: Fix Carbon; DT: Distortion Temperature; ST: Soften Temperature; HT: Hemispherical Temperature; FT: Flow Temperature.

2.1.3. Additive

The additive of sodium sulfate is of analytical reagent (AR) grade, which is used to enhance reduction of iron oxide and growth of grain size of element iron.

2.1.4. Flux

CaO powder of analytic grade was used as flux in this work to adjust the binary basicity (ratio of CaO/SiO2) of the mixture, and its particle size is less than 74 μm.

2.2. Experimental Methods

2.2.1. High Temperature Flash Reduction

The oolitic hematite ore was sufficiently mixed manually for approximate 15 min with a certain proportion of additives, flux and coal according to the required amount. Then the uniformly mixed raw materials were let into cylinders with a diameter of 10 mm and height of 10 mm to form briquettes, subsequently being dried at 105 °C for at least 3 h in a drying oven. After that, about 55 g of dry briquettes were loaded into an alumina crucible. When the temperature of the $MoSi_2$ electric furnace reached the fixed value, the briquettes were charged into the furnace rapidly and then were reduced for predetermined time. After reducing, the alumina crucible was taken out from the furnace and the reduced briquettes in the alumina crucible were cooled down to ambient temperature under the protection of nitrogen for the subsequent beneficiation process.

2.2.2. Magnetic Separation

Prior to grinding, reduced briquettes were crushed to a particle size below 1 mm. Then, a 20 g batch of sample (as crushed) was mixed with 20 mL of water and ground in a small stainless steel ball mill (model: XMQ240 × 90). The grinding fineness was controlled by adjusting the grinding time. Subsequently, the mix slurry was dressed by one-stage wet magnetic separation for 10 min in an XCGS-73 Davies Magnetic Tube (model: XCGS-73, Changsha Research Institute of Mining and Metallurgy Co., Changsha, China) at a magnetic field strength in the range of 0.06–0.10 T. The products were dried at 75 °C in a vacuum oven for 2 h. After that, the compositions of both dry magnetic and non-magnetic products were analyzed using chemical methods.

2.2.3. Analytic Tests

The crystallization phase composition of samples was investigated using an X-ray diffractometer (XRD, D/Max-2500, RIGAKU, Tokyo, Japan). Microstructures of reduced briquettes were identified using Leica DMLP optical microscopy (Leica Company, Wetzlar, Germany), an FEI Quata-200 scanning electron microscope (FEI Company, GG Eindhoven, The Netherlands) and an EDAX32 genesis spectrometer (Ametek Inc., Paoli, PA, USA). SEM images were recorded in backscatter electron modes operating in low vacuum mode at 0.5 Torr and 20 keV [16].

2.3. Evaluation Indexes

The reduction results were assessed by iron grade and phosphorus content of magnetic products, iron metallization degree of reduced briquettes, iron recovery and phosphorus removal rate of the magnetic separation process, and those indexes were calculated as follows:

Iron metallization degree of reduced briquettes:

$$\eta_{Fe} = \frac{MFe}{TFe_1} \times 100\%$$

where η_{Fe} is iron metallization degree of reduced briquettes; MFe is metallic iron content of reduced briquettes; TFe_1 is total iron grade of reduced briquettes.

Iron recovery of magnetic separation:

$$\varepsilon = \frac{TFe_2 \times m_2}{TFe_1 \times m_1} \times 100\%$$

where ε is iron recovery of magnetic separation; TFe_1 is total iron grade of reduced briquettes; TFe_2 is total iron grade of magnetic product; m_1 is the mass of dried reduced briquettes feeding for magnetic separation; m_2 is the mass of dried magnetic product of magnetic separation.

Phosphorus removal rate of magnetic separation:

$$R_P = \left(1 - \frac{P_2 \times m_2}{P_1 \times m_1}\right) \times 100\%$$

where R_p is phosphorus removal rate of magnetic separation; P_1 is phosphorus content of reduced briquettes; P_2 is phosphorus content of magnetic product of magnetic separation; m_1 is the mass of dried reduced briquettes feeding for magnetic separation; m_2 is the mass of dried magnetic product of magnetic separation.

Image analysis is a technique that is used to measure the particle size of metallic iron in the reduced ore, and the detail methods could be referred the literature [17]. The shape of metallic iron particle was assumed as sphere, and the particle size of metallic iron was calculated as:

$$D = 2 \times \sqrt{\frac{S}{\pi \times N}}$$

where S is the areas of metallic iron particles; N is the numbers of metallic iron particles.

3. Results and Discussion

3.1. Thermodynamic Analysis

3.1.1. Thermodynamic Analysis of Iron Mineral Reactions in the Reduction

Many previous works has reported the reduction of pure hematite proceeds stepwise ($Fe_2O_3 \rightarrow Fe_3O_4 \rightarrow FeO \rightarrow Fe$) at a temperature higher than 570 °C. However, when the SiO_2 or Al_2O_3 exists in the iron ores, the thermodynamic conditions are somewhat changed and their reduction behaviors vary accordingly.

$$SiO_2 + 2FeO = Fe_2SiO_4 \quad (1)$$

$$l_2O_3 + FeO = FeO{\cdot}\,Al_2O_3 \quad (2)$$

In case of adjusting the basicity and adding the sodium sulfate in the reduction system, the most likely reduction reactions take place as follows:

$$Fe_2SiO_4 + 2C = 2Fe + SiO_2 + 2CO \quad (3)$$

$$Fe_2SiO_4 + 2CaO + 2C = Ca_2SiO_4 + 2Fe + 2CO \quad (4)$$

$$Fe_2SiO_4 + Na_2SO_4 + 5C = Na_2SiO_3 + 2Fe + FeS + 5CO \quad (5)$$

$$FeO{\cdot}\,Al_2O_3 + C = Fe + Al_2O_3 + CO \quad (6)$$

$$FeO{\cdot}\,Al_2O_3 + CaO + C = CaAl_2O_4 + Fe + CO \quad (7)$$

$$2FeO{\cdot}\,Al_2O_3 + 2Na_2SO_4 + 8C = 4NaAlO_2 + Fe + FeS + 8CO \quad (8)$$

Stand Gibbs energy changes of Equations (1)–(7) are plotted in Figure 4. It is noted that in the presence of burnt lime or sodium sulfate, the stand Gibbs free energy for reduction reaction of fayalite (Fe_2SiO_4) and hercynite ($FeAl_2O_4$) is lower than the other reactions in the tested temperature rang. That implies that adding an appropriate amount of sodium sulfate or burnt lime can promote the reduction of iron minerals thermodynamically.

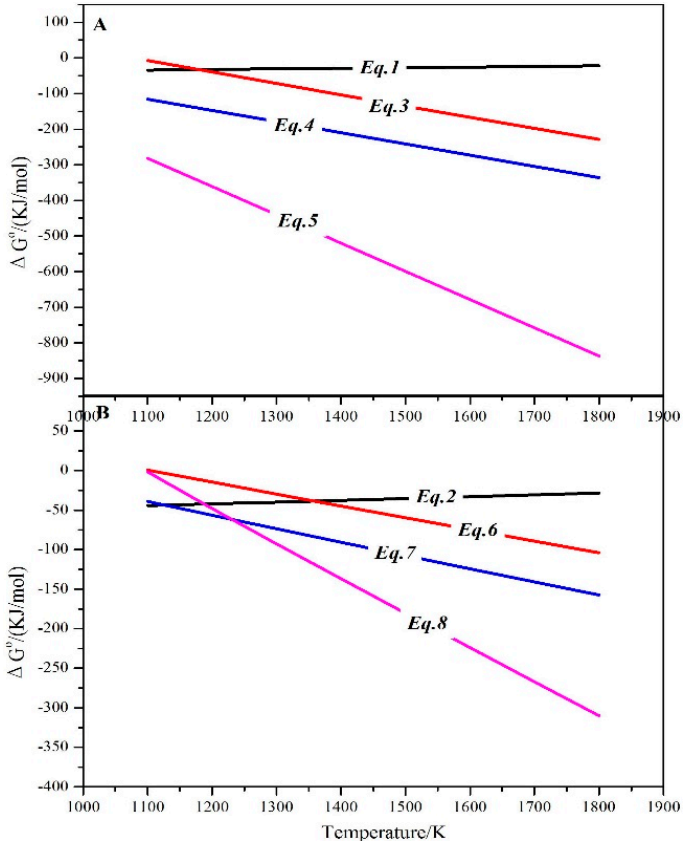

Figure 4. Relationships of reduction roasting reactions of iron minerals. (**A**) Reduction of Fe_2SiO_4; (**B**) reduction of $FeAl_2O_4$.

3.1.2. Thermodynamic Analysis of Phosphorus Mineral Reactions in the Reduction

Phosphorus in high-phosphorus hematite ore occurs in the form of apatite ($Ca_3(PO_4)_2$). When the coal is induced to the direct reduction process, iron minerals in the sample can be reduced to metallic iron by the carbon. Meanwhile, apatite also could be reduced by reaction with additives and gangue minerals during the reducing roasting. The possible reactions are as follows:

$$Ca_3(PO_4)_2 + 5C = 3CaO + P_2 + 5CO \quad (9)$$

$$Ca_3(PO_4)_2 + 6SiO_2 + 3Al_2O_3 + 5C = 3CaAl_2Si_2O_8 + P_2 + 5CO \quad (10)$$

$$2SiO_2 + Al_2O_3 + Na_2SO_4 + C = 2NaAlSiO_4 + SO_2 + CO \quad (11)$$

$$2SiO_2 + Al_2O_3 + CaO = CaAl_2Si_2O_8 \quad (12)$$

Figure 5 illustrates the relationships of stand Gibbs free energy and temperatures for reactions between apatite, sodium sulfate and gangue minerals. It is clear that individual apatite is very difficult to reduce, whereas if SiO_2 and Al_2O_3 exist, the reduction of apatite would be improved. In addition, Na_2O and CaO reacts with Al_2O_3 and SiO_2 more easily than with apatite, which means Al_2O_3 and SiO_2 are preferentially consumed by sodium sulfate and burnt lime, thereby inhibiting the reduction of apatite and removal of phosphorus. Therefore, much more sodium sulfate or burnt lime is required to improve the reduction of iron ores and removal of phosphorus.

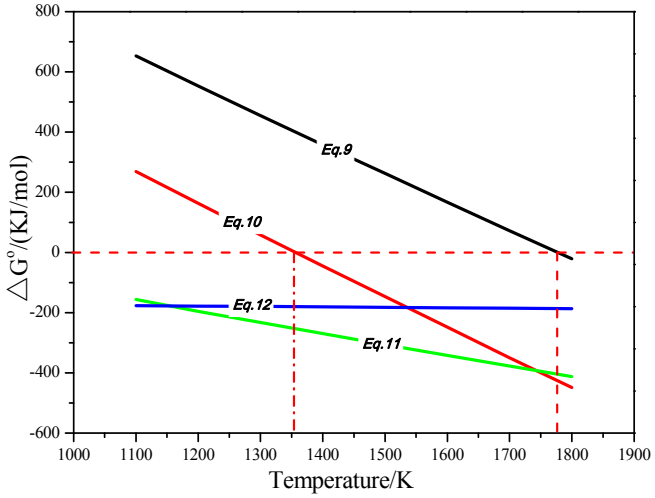

Figure 5. Correlation of standard free energy with temperature for Equations (9)–(12).

3.2. High Temperature Quick Reduction

The raw briquettes were subjected to quick reduction at high temperatures, and then the reduced briquettes were separated by wet-magnetic separation. The grinding fineness of reduced briquettes was about 98% over 0.074 mm and the magnetic field intensity was fixed at 0.1 T.

3.2.1. Effects of C/Fe (Mass Ratio)

The effects of C/Fe on beneficiation of iron and phosphorus removal are presented in Figure 6. It shows that with the C/Fe increasing from 0.24 to 0.48, the iron metallization degree of reduced briquettes, iron grade of magnetic material and iron recovery were increased significantly. When the C/Fe was beyond 0.48, the iron grade tended to decrease. On the other hand, the phosphorus removal rate of magnetic separation dropped noticably with an increase in C/Fe, whereas the phosphorus content of magnetic products was decreased significantly to the lowest value of 0.18% during the initial addition of C/Fe mass ratio to 0.36 then increased rapidly.

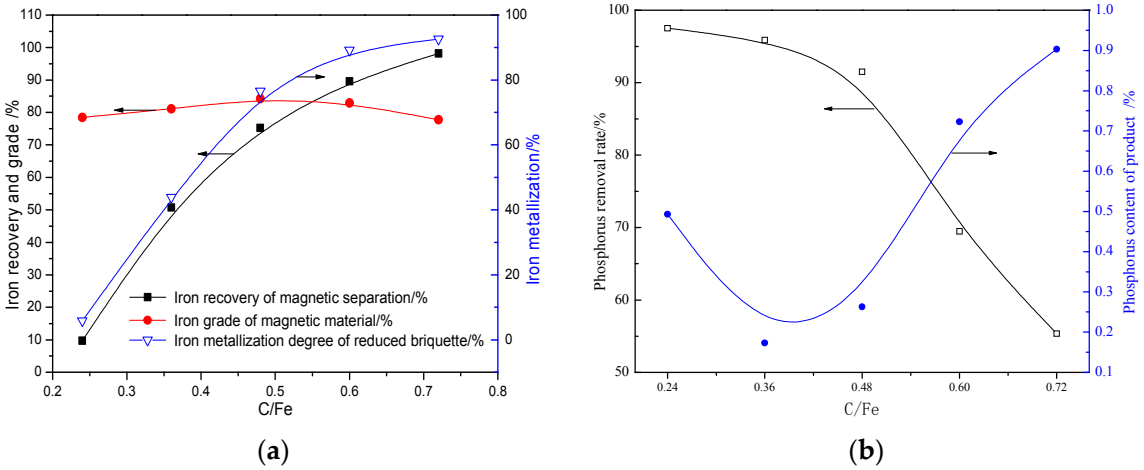

Figure 6. Effects of C/Fe (mass ratio) on beneficiation of iron and phosphorus removal rate (2.4 basicity, ore blended with 10% sodium sulfate and reducing at 1350 °C for 15 min). (**a**) Effect of C/Fe on iron recovery; (**b**) effect of C/Fe on phosphorus removal.

Generally, with the addition of soft coal, the Boundouard reaction was accelerated to produce more CO, leading to a stronger reducing atmosphere and promoting hematite reduction. However,

with a further increase in C/Fe, more apatite was reduced to P_2 gas, and then the generated P_2 could dissolve into metallic iron to form Fe-P solid solution [18]. As a result, the phosphorus content of magnetic product was increased, and the phosphorus removal rate of magnetic separation declined. Therefore, the optimum recommended C/Fe mass ratio is at 0.48.

3.2.2. Effects of Reduction Temperature

The plot in Figure 7 shows the effects of reduction temperature on beneficiation of iron and phosphorus removal rate. With the increase of the reduction temperature from 1200 °C to 1300 °C, the iron grade of magnetic material, iron recovery and phosphorus removal rate of magnetic separation increased significantly, whereas the iron metallization degree of reduced briquette and phosphorus content of magnetite materials decreased simultaneously.

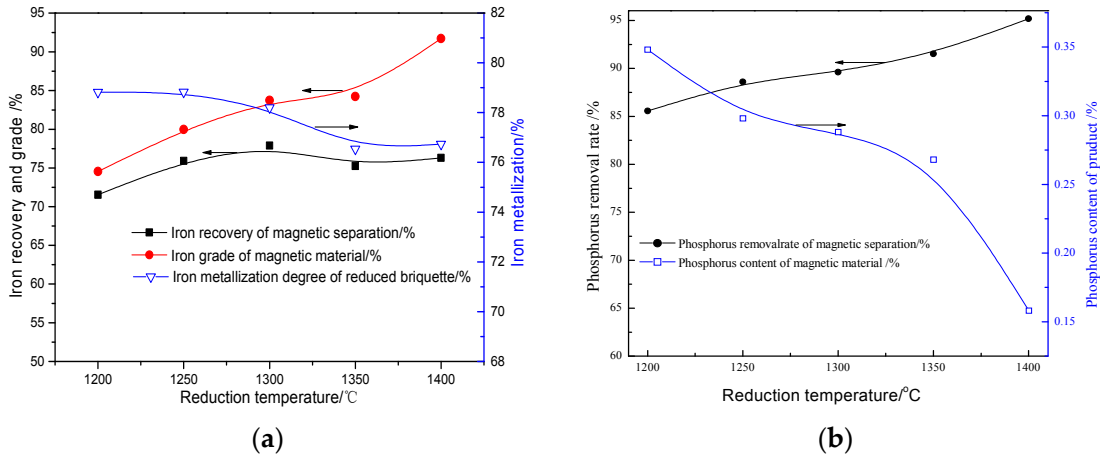

Figure 7. Effects of reduction temperature on beneficiation of iron and phosphorus removal (2.4 basicity, ore blended with 10% sodium sulfate and reducing for 15 min with C/Fe = 0.48). (**a**) Effect of temperature on iron recovery; (**b**) effect of temperature on phosphorus removal.

This effect may be explained by the fact that increasing moderately the temperature will destroy the oolitic structure, enhance the reduced process of iron-bearing minerals and promote iron grain growth, thereby improving separation between iron and phosphorus as well as beneficiation of iron. However, if the reduction temperature was above 1300 °C, the iron recovery of magnetic separation and iron metallization of reduced briquettes tended to decline. This is due to the fact that the reactions between FeO and silica and aluminum would be improved to form more low smelting point minerals, such as fayalite, which impeded the internal diffusion of reducing gas in the direct reduction process once the reduction temperature was excessively high [19]. Moreover, it is of particular concern, as the reduction temperature is over 1350 °C, the reduced briquettes would be melted, leading to destruction of normal appearance structures. In conclusion, the recommended temperature is 1350 °C.

3.2.3. Effects of Reduction Duration

The effects of reduction duration varied from 10 min to 20 min on recovery of iron and phosphorus removal are shown in Table 5.

With an increase of the reduction time from 5 to 10 min, the iron recovery, iron grade and iron metallization degree were improved significantly. Prolonging the reduction duration further from 10 to 20 min, the iron grade and phosphorus content of magnetic material tended to decline slightly, phosphorus removal rate of magnetic separation increased gradually from 89.03% to 93.02%, and the iron recovery and iron metallization dropped conspicuously. It was inferred that 10 min was sufficient for the reduction of iron minerals, growth and aggregation of metallic iron grains in the high temperature flash reduction process. When the reduction duration further extended, the reduction

agent would be rapidly exhausted at this high temperature, resulting in weakening of reducing atmosphere. Thereby, the generated metallic iron would be subjected to re-oxidation, which can be confirmed by the decrease of metallization degree of reduced briquettes. Consequently, from a practical point of view, the recommended reducing duration is 10 min, which is a real flash reduction process.

Table 5. Effects of reduction duration on phosphorus removal and magnetic separation.

Reduction Duration/min	Metallization Degree/%	Magnetic Product		Iron Recovery/%	Phosphorus Removal Rate/%
		TFe/%	P/%		
5	76.32	77.32	0.33	72.23	83.76
10	86.92	86.02	0.29	89.69	89.03
15	76.54	84.24	0.27	75.25	91.51
20	69.59	83.56	0.25	63.57	93.02

2.4 basicity, ore blended with 10% sodium sulfate and reducing at 1350 °C with C/Fe = 0.48.

3.2.4. Effects of Basicity

The influence of basicity on beneficiation of iron and dephosphorization are shown in Figure 8, indicating that when the basicity was raised from 0.48 (natural basicity) to 3.2, the iron grade and iron recovery were increased gradually up to the peak value of 90.02% and 91.56% respectively at 1.6 basicity, then declined obviously. The iron metallization degree were decreased gradually in the whole range of tested basicity. Meanwhile, owing to the increase of basicity, the removal of phosphorus was improved. When the basicity was beyond 2.4, the phosphorus removal rate of magnetic separation and phosphorus content of magnetic product remained steady.

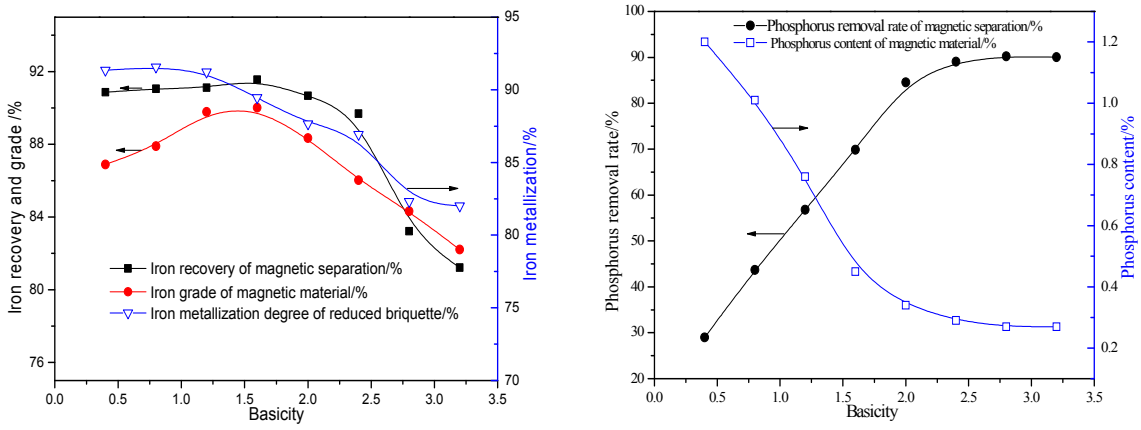

Figure 8. Effects of basicity on beneficiation of iron and phosphorus removal (ore blended with 10% sodium sulfate and reducing at 1350 °C for 10 min with C/Fe = 0.48). (**a**) Effect of basicity on iron recovery; (**b**) effect of basicity on phosphorus removal.

The proper addition of burnt lime would improve the reduction of FeO since CaO is easier to combine with SiO_2 and Al_2O_3. However, at a higher basicity, with much more burnt lime added to the iron ore, the distance between the iron particles increased, which was unfavorable for the aggregation and growth of metallic iron grains. In the meantime, more high-melting-point substances were generated at higher basicity, such as $CaSiO_3$, Ca_2SiO_4, and the fraction of liquid phases would be reduced, which were negative for diffusion of metallic iron grains. As a result, the recovery of iron is correspondingly inhibited.

Conversely, the increase of basicity is rewarding to the removal of phosphorus. Han *et al.* pointed out the beginning reduction temperature of apatite increased with increasing basicity according to the thermodynamic data for reduction of apatite with burnt lime [20]. That is, the higher basicity restrains the reduction of apatite and the generation of P_2, thereby reducing the probability of formation of Fe-P, which can improve the phosphorus removal rate of the samples. Moreover, at a higher basicity, the generated dicalcium silicate (Ca_2SiO_4) can immobilize P, because some P may dissolve into a lattice of dicalcium silicate to form solid solution ($Ca_{2-x/2}Si_{1-x}P_xO_4$), which is easy to remove by magnetic separation.

Additionally, as seen in Figure 9, when the basicity is lower than 2.0, the briquettes were smelted and normal appearance structure of the reduced briquettes was broken, due to superabundant liquid phase generated. Therefore, the recommended optimum basicity is 2.4.

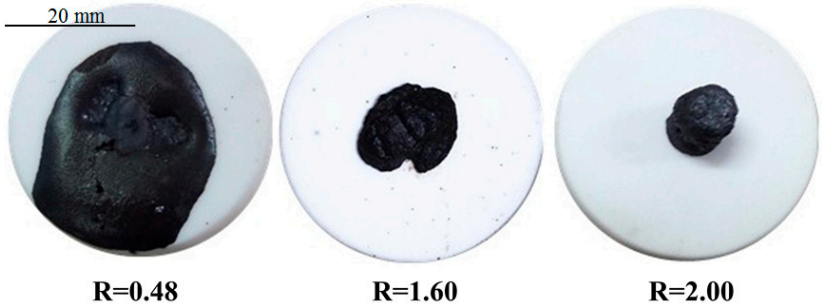

Figure 9. Appearance of the reduced briquette at different basicity (R = the ratio of CaO to SiO_2) (Ore blended with 10% sodium sulfate and reducing at 1350 °C for 10 min with C/Fe = 0.48).

3.2.5. Effects of Sodium Sulfate Dosage

The effects of sodium sulfate dosage on reduction and phosphorus removal presented in Figure 10 show that with an increase in sodium sulfate dosage from 0 to 15%, the iron metallization degree of reduced briquettes and iron recovery of magnetic separation changed slightly, but iron grade of magnetic product increased obviously from 70.72% to 88.01%. However, with addition of more sodium sulfate, the metallization degree and iron recovery dropped sharply. On the contrary, the phosphorus removal rate of magnetic separation increased significantly with an increase in dosage of sodium sulfate, along with phosphorus content of magnetic product declining markedly from 0.78% to 0.22%.

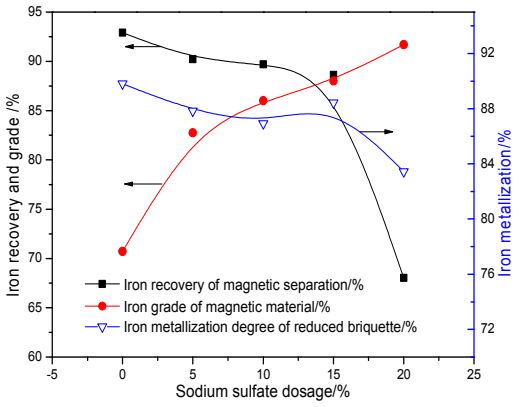

(**a**) Effect of sodium sulfate dosage on iron recovery

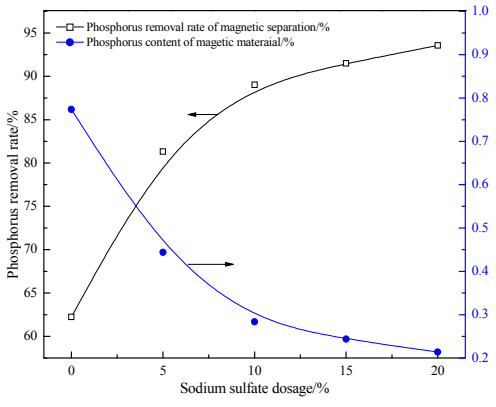

(**b**) Effect of sodium sulfate dosage on phosphorus removal

Figure 10. Effects of sodium sulfate dosage on beneficiation of iron and phosphorus removal (2.4 basicity and reducing at 1350 °C for 10 min with C/Fe = 0.48). (**a**) Effect of sodium sulfate dosage on iron recovery; (**b**) effect of sodium sulfate dosage on phosphorus removal.

The results imply that properly increasing the sodium sulfate dosage is favorable to enhance the beneficiation of iron and removal of phosphorus. In the presence of sodium sulfate, Na_2O, formed from decomposition of Na_2SO_4, can preferentially participate in the reaction with SiO_2 and Al_2O_3 in gangue minerals, thereby inhibiting generation of fayalite ($2FeO\cdot SiO_2$) and hercynite ($FeO\cdot Al_2O_3$), which are difficult to reduce. Thus, more FeO is reduced to metallic iron, and the reduction of iron oxide is enhanced. Moreover, owing to the presence of sodium sulfate, a certain amount of FeS would be generated in the reducing process, which will react with Fe to form Fe-FeS solid solution possessing a lower melting point, resulting in the formation of some liquid phase and accelerating metallic iron grains aggregation via this "liquid phase bridge" [14]. As shown in Table 6 the content of element S in the iron powder is 0.10%, which may indicate some Fe-FeS solid solution exists. Some research also revealed that Na_2O can promote the transport of electrons from Fe^{3+} to Fe^0 during the reduction, improving the reduction of iron oxides [21].

Table 6. Chemical composition of metallic iron powder/%.

TFe	SiO_2	Al_2O_3	CaO	MgO	Na_2O	P	S
91.12	2.13	0.27	0.79	0.54	0.35	0.25	0.10

Meanwhile, since sodium sulfate has the capacity to react with gangue minerals (SiO_2, Al_2O_3) in advance, the reduction of apatite was restrained, and the phosphorus removal was significantly improved by injecting apatite into tailings in magnetic separation, as shown in the thermodynamic analysis of reduction of apatite.

Based on the multiple effects of sodium sulfate, the beneficiation of iron and phosphorus removal was enhanced simultaneously. However, the unfavorable impact of excessive sodium sulfate on quality of magnetic product should not be neglected, such as lower iron grade and higher S content, due to too much FeS formation, which suppresses metallization of iron [15]. Thus, the proper sodium sulfate dosage is recommended at 15.0%.

3.3. Magnetic Separation of Reduced Products

The effects of grinding fineness and magnetic field on the upgrading of iron and phosphorus removal is presented in Table 7. It is shown that the magnetic concentrate (metallic iron powder), assaying total iron grade of 91.12% and phosphorus content of 0.25%, was obtained at 90.08% iron recovery under the conditions of grinding the reduced briquettes up to 95.72% over 0.074 mm, and magnetically separating the ground product in a Davi Tube at 0.10 T magnetic field intensity.

Table 7. Effects of the grinding-separation process on upgrading of iron and phosphorus removal.

Grinding Fineness (−0.074 mm/%)	Magnetic Field Intensity/T	Magnetic Product		Iron Recovery/%	Phosphorus Removal Rate/%
		TFe/%	P/%		
88.49	0.06	89.45	0.26	82.30	91.91
	0.08	83.75	0.32	86.29	88.85
	0.10	85.70	0.29	83.51	90.44
95.72	0.06	89.36	0.23	89.20	93.11
	0.08	88.78	0.24	88.26	92.48
	0.10	91.12	0.25	90.08	91.79
97.86	0.06	89.37	0.27	79.30	91.90
	0.08	90.16	0.23	77.40	93.32
	0.10	88.01	0.25	88.63	91.49

2.4 basicity and 15% sodium sulfate, reducing at 1350 °C for 10 min with C/Fe = 0.48.

3.4. Analysis of Final Product

Through the above experiments, a satisfactory product was obtained under the conditions of briquetting the ore mixture with 2.4 basicity and 15% sodium sulfate and reducing briquettes at 1350 °C for 10 min with C/Fe mass ratio of 0.48, and then grinding the reduced briquettes up to 95.72% over 0.074 mm, and a magnetic separation at 0.1 T. The chemical composition of metallic ferrous powder is shown in Table 7. The iron grade of metallic iron powder is higher than 91% and other impurities, such as the content of sulfur and phosphorus, are a little higher. The briquettes of metallic iron powder can be used as the burden for steel-making by electric arc furnace to replace scrap steel parts.

3.5. Mechanism of Removal of Phosphorus and Beneficiation of Iron

3.5.1. Phase Transformation of Oolitic Hematite Ore During Reduction Process

In order to find out the mechanism of phosphorus removal beneficial for oolitic hematite by high temperature flash reduction, XRD analysis was carried out to reveal the difference in mineral compositions between two kinds of reduced briquettes. The results are shown in Figure 11.

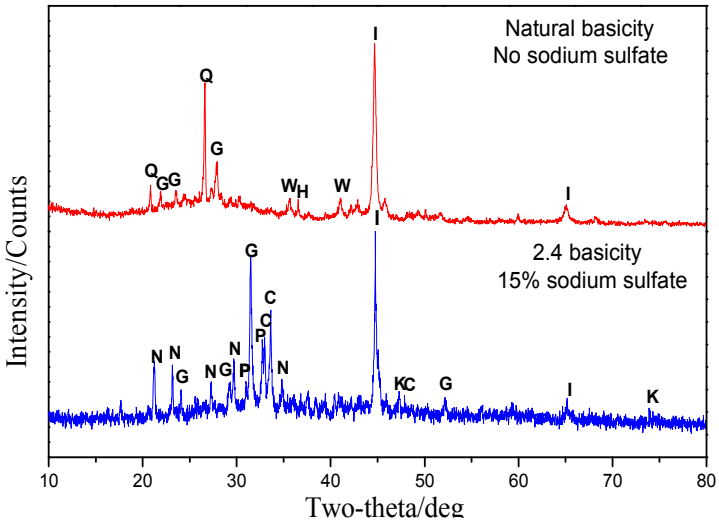

Figure 11. X-ray diffraction pattern of the reduced briquettes. Q-SiO_2; G-$CaAl_2Si_2O_8$; W-FeO; H-FeO· Al_2O_3; I-Fe; P-$Ca_3(PO_4)_2$; N-$NaAlSiO_4$; C-Ca_2SiO_4; K-$CaAl_2O_4$. Reducing at 1350 °C for 10 min with C/Fe mass ratio of 0.48.

It can be seen from Figure 11 that when no sodium sulfate and burnt lime was added in the iron ore, the iron phase mainly existed in metallic iron, and the minor iron occurred in hercynite (FeO· Al_2O_3) and wüstite (FeO); meanwhile the gangue minerals presented primarily in quartz (SiO_2) and minor gehlenite ($CaAl_2Si_2O_8$). With the addition of burnt lime and sodium sulfate in the iron ore, the peaks of wüstite, hercynite and quartz were vanished, while the new phases, such as nepheline ($NaAlSiO_4$) and calcium silicate (Ca_2SiO_4), were detected, and the original peak of gehlenite ($CaAl_2Si_2O_8$) was enhanced. This is because that sodium sulfate and burnt lime can readily react with Al_2O_3 and SiO_2 instead of apatite to form the $NaAlSiO_4$ and $CaAl_2Si_2O_8$ (Equations (11) and (12)), leading to the disappearance of quartz (SiO_2) and conservation of apatite. Thus, these results agreed well with the thermodynamic analysis mentioned above.

3.5.2. Growth of Metallic Iron Grains in Reduction

The two types of reduced briquettes without sodium sulfate and with 15% sodium sulfate were prepared by reducing at 1350 °C for 10 min with 2.4 basicity and C/Fe of 0.48, and the microstructures are shown in Figure 12.

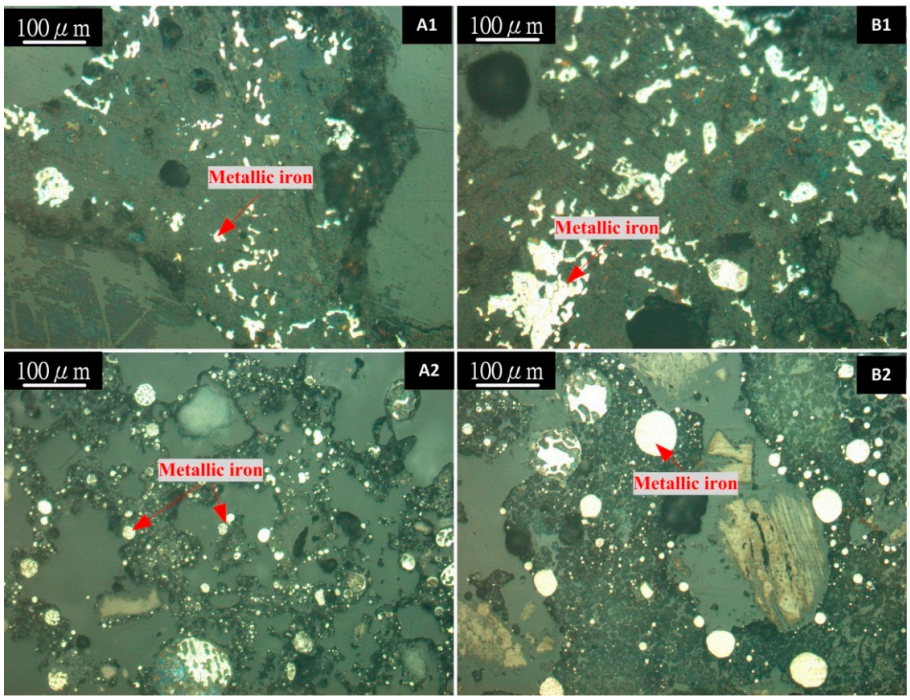

Figure 12. Microstructures of reduced briquettes. (**A1**,**A2**) External and internal of reduced briquettes without sodium sulphate. (**B1**,**B2**) External and internal of reduced briquettes with 15% sodium sulfate.

As shown in Figure 12A1,2, although many bright white metallic iron grains can be observed, they were very fine and dispersive in reduced briquette in the absence of sodium sulfate, and most of them ranged between 5 and 15 μm in size. In contrast, it can be seen from Figure 12B1,2 that the metallic iron grains in the briquettes with 15% sodium sulfate aggregated together and increased in size. In order to quantitatively describe the growth of metallic iron grains, the average grain size of metallic iron of reduced briquettes with different amounts of sodium sulfate was calculated and the results are presented in Figure 13.

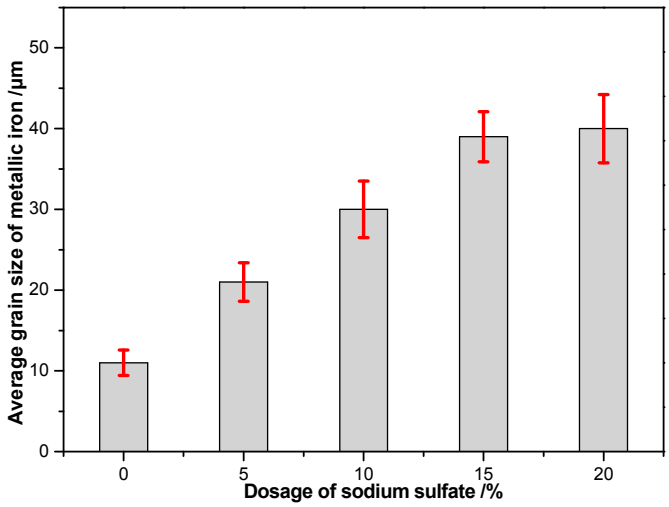

Figure 13. Effect of sodium sulfate dosage on the grain size of metallic iron (Reducing at 1350 °C for 10 min with 2.4 basicity and C/Fe = 0.48).

As shown in Figure 13, the average grain size of metallic iron of reduced briquettes increased significantly from 11 to 39 μm when the dosage of sodium sulfate was added from 0 to 15%, and then

kept steady, indicating that the sodium sulfate is well-suited to cause the metallic iron to reshape and coalesce. Generally, the larger size of the minerals responds very well to sufficient liberation in the milling process and subsequent physical separation. Therefore, the iron was upgraded at higher iron recovery, and the phosphorus content of metallic iron powder was decreased by the magnetic separation at the higher removal rate of phosphorus.

To identify the phase in the reduced briquettes, EDS analysis was performed in the regions marked in the SEM image shown in Figure 14 and the element content of different points in SEM is given in Table 8. In the slag, the Fe content of point A1 was still higher than 13% whereas the P content was very low in the slags, which indicated that the many superfine metallic iron grains had not grown, while a considerable amount apatite had been reduced to P_2 in the absence of sodium sulfate. In contrast, from the Figure 14B, the Fe content of point B1 was only 1.81% and the corresponding P content reached 5.21%, which implied the phosphorus mainly enriched in the slag, so the beneficiation of iron and phosphorus removal were improved. In the metallic iron, the P content of point A2 was as high as 0.78%, indicating that the apatite in the ore was reduced and the generated phosphorus entered into the metallic iron grains, while the metallic iron grains contained a relatively low level of phosphorus in the briquettes with 15% sodium sulfate, even not detected (as shown in point B2), which further confirms that the sodium sulfate is favorable to the removal of phosphorus.

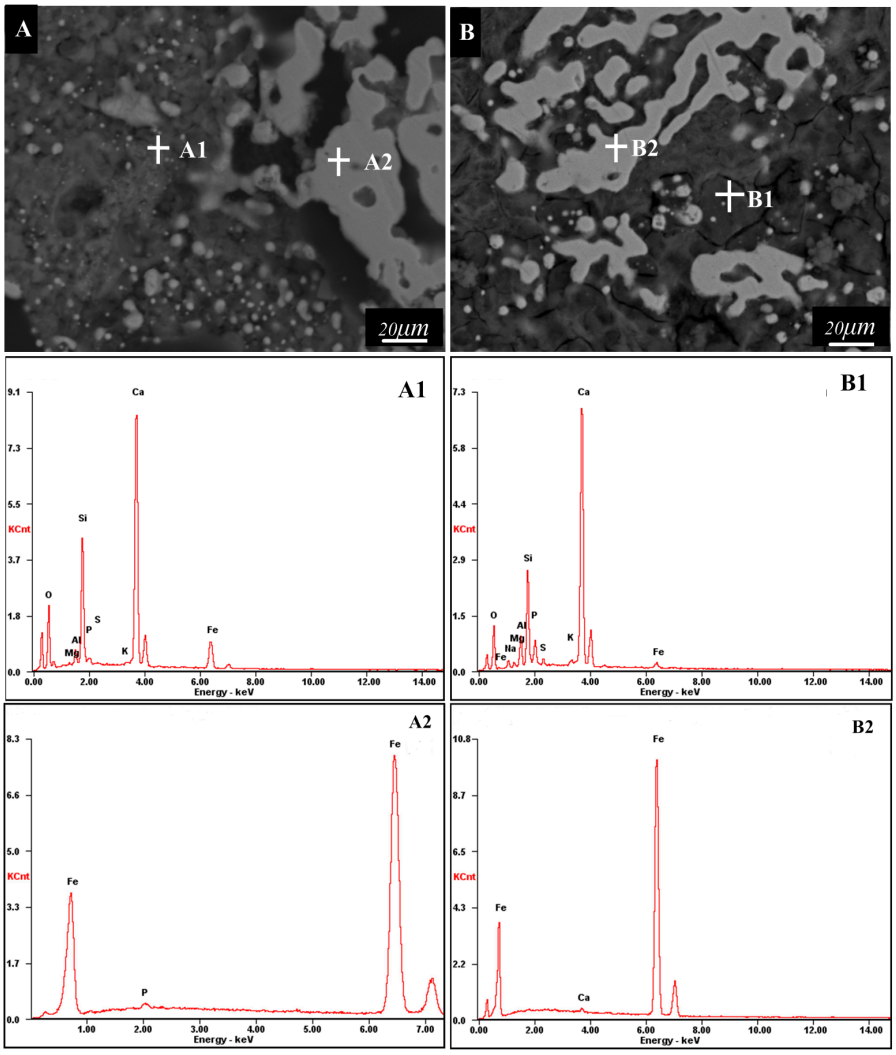

Figure 14. SEM-EDS image of reduced briquettes in the absence and presence of Na_2SO_4 (reducing at 1350 °C for 10min with 2.4 basicity and C/Fe = 0.48). (**A**) No sodium sulfate; (**B**) 15% sodium sulfate.

Table 8. Element content of different points in SEM.

Element		OK	MgK	AlK	SiK	PK	SK	KK	CaK	FeK	NaK
A1	Wt%	28.72	0.28	1.63	13.60	0.88	0.18	0.53	40.94	13.25	/
	At%	49.08	0.31	1.65	13.24	0.78	0.15	0.37	27.93	6.49	/
B1	Wt%	24.83	0.93	2.44	10.80	5.21	3.93	1.15	44.67	1.81	4.23
	At%	41.76	1.03	2.43	10.35	4.53	3.30	0.79	29.99	0.87	4.96
A2	Wt%	/	/	/	/	0.78	/	/	/	99.22	/
	At%	/	/	/	/	1.39	/	/	/	98.61	/
B2	/	/	/	/	/	/	/	/	0.45	99.55	/
	/	/	/	/	/	/	/	/	0.63	99.37	/

4. Conclusions

The feasibility of an integrated technological route to improve separation of Fe and P from high-phosphorus oolitic hematite ore through high-temperature reduction and wet magnetic separation was investigated, and the conclusions below were reached:

1. Oolitic hematite ore, assaying 41.50% Fe_{total}, 1.24% P, 17.04%Al_2O_3 and 4.68% SiO_2, was used as a raw material to produce metal iron powder. The characterization of the sample in mineralogy indicates that phosphorus appears mainly in calcium phosphate, and the main iron-bearing mineral, hematite, is superfinely disseminated and combined closely with other gangue minerals, resulting in poor beneficiation of iron and phosphorus removal by traditional dressing process.
2. The quick high-temperature reduction process was conducted to improve the separation of Fe and P with the optimized conditions briquetting the ore mixture with 15% sodium sulphate and 2.4 basicity, and reducing at 1350 °C for 10 min with C/Fe of 0.48. The reduced briquettes obtained were then subjected to wet magnetic separation under the conditions of grinding at 95.72% over 0.074 mm, and magnetically separating the ground product in a Davi Tube at 0.10 T, and the final product (metallic iron powder), assaying 91.12% Fe_{total} and 0.25% P, was produced at overall iron recoveries of 90.08%, which can be used as the burden for steel-making.
3. CaO and Na_2SO_4 can preferentially participate in the reactions with SiO_2 and Al_2O_3, suppressing the reduction of calcium phosphate and intensifying the phosphorus removal. Meanwhile, sodium sulfate is suited to promoting the aggregation and growth of metallic iron grains, resulting in the elevation of the iron grade and recovery in the magnetic separation process.

Acknowledgments: The authors wish to express their thanks to the National Torch Program Projects of China (2011GH561685) for the financial support of this research.

Author Contributions: D.Z., Z.G. and J.P. conceived and designed the experiments; Z.G. and F.Z. performed the experiments; Z.G. wrote the paper; D.Z. and J.P. modified the paper.

Conflicts of Interest: The authors declare no conflict of interest.

References

1. Cheng, C.Y.; Misra, V.N.; Clough, J.; Muni, R. Dephosphorisation of Western Australian iron ore by hydrometallurgical process. *Miner. Eng.* **1999**, *12*, 1083–1092. [CrossRef]
2. Li, K.Q.; Ni, W.; Zhu, M.; Zheng, M.J.; Li, Y. Iron extraction from oolitic iron ore by a deep reduction process. *J. Iron Steel Res. Int.* **2011**, *18*, 9–13. [CrossRef]
3. Forssberg, E.; Adolfsson, G. Dephosphorization of high phosphorus ores by acid leaching. *J. Explor. Min. Metall.* **1981**, *34*, 316–322.
4. Jiang, T.; Jin, Y.S.; Li, Q.; Yang, Y.B.; Li, G.H.; Qiu, G. Dephosphorization technology of iron ores by Acidthiobacillus ferrooxidans. *Chin. J. Nonferrous Met.* **2007**, *17*, 1718–1722.
5. Muhammed, M.; Zhang, Y. A hydrometallurgical process for the dephosphorization of iron ore. *Hydrometallurgy* **1989**, *21*, 277–292. [CrossRef]

6. Delvasto, P.; Valverde, A.; Ballester, A.; Muñoz, J.; González, F.; Blázquez, M.; Igual, J.; García-Balboa, C. Diversity and activity of phosphate bioleaching bacteria from a high-phosphorus iron ore. *Hydrometallurgy* **2008**, *92*, 124–129. [CrossRef]
7. Priha, O.; Sarlin, T.; Blomberg, P.; Wendling, L.; Mäkinen, J.; Arnold, M.; Kinnunen, P. Bioleaching phosphorus from fluorapatites with acidophilic bacteria. *Hydrometallurgy* **2014**, *12*, 269–275. [CrossRef]
8. Tariq, M.B.; Wasim, Y. Bacterial solubilization of phosphorus from phosphate rock containing sulfur-mud. *Hydrometallurgy* **2014**, *103*, 54–59.
9. Matinde, E.; Hino, M. Dephosphorization treatment of high phosphorus iron ore by pre-reduction, air jet milling and screening methods. *ISIJ Int.* **2011**, *51*, 544–551. [CrossRef]
10. Wu, Y.; Zhang, Y.S.; Liu, Y.C. Flotation research on a high phosphorus-bearing oolitic hematite ore in Erxi. *China Min. Mag.* **2011**, *11*, 71–86.
11. Yin, J.Q.; Lv, X.W.; Bai, C.G.; Qiu, G.B.; Ma, S.W.; Xie, B. Dephosphorization of iron ore bearing high phosphorous by carbothermic reduction assisted with microwave and magnetic separation. *ISIJ Int.* **2012**, *52*, 1579–1584. [CrossRef]
12. Yu, W.; Sun, T.C.; Kou, J.; Wei, Y.X.; Xu, C.Y.; Liu, Z.Z. The Function of $Ca(OH)_2$ and Na_2CO_3 as additive on the reduction of high-Phosphorus oolitic hematite-coal mixed pellets. *ISIJ Int.* **2013**, *53*, 427–433. [CrossRef]
13. Bai, S.J.; Wen, S.M.; Liu, D.W.; Zhang, W.B.; Cao, Q.B. Beneficiation of high phosphorus limonite ore by sodium carbonate-added carbothermic reduction. *ISIJ Int.* **2012**, *52*, 1757–1763. [CrossRef]
14. Li, G.H.; Zhang, S.H.; Rao, M.J.; Zhang, Y.B.; Jiang, T. Behavior of phosphorus during the carbothermic reduction of phosphorus-rich oolitic hematite ore in the presence of Na_2SO_4. *Int. J. Miner. Process.* **2015**, *124*, 26–34. [CrossRef]
15. Li, Y.L.; Sun, T.C.; Xu, C.Y.; Liu, Z.H. New dephosphorizing agent for phosphorus removal from high-phosphorus oolitic hematite ore in direct reduction roasting. *J. Cent. South Univ. Sci. Technol.* **2012**, *43*, 827–834.
16. Guo, Z.Q.; Zhu, D.Q.; Pan, J.; Wu, T.J.; Zhang, F. Improving beneficiation of copper and iron from copper slag by modifying the molten copper slag. *Metals* **2016**. [CrossRef]
17. Zhu, D.Q.; Chun, T.J.; Pan, J.; Zhang, J.L. Influence of basicity and MgO content on metallurgical performances of Brazilian specularite pellets. *Int. J. Miner. Process.* **2013**, *125*, 51–60. [CrossRef]
18. Zhou, X.L.; Zhu, D.Q.; Jian, P.; Luo, Y.H.; Liu, X.Q. Upgrading of high-aluminum hematite-limonite ore by high temperature reduction-wet magnetic separation process. *Metals* **2016**, *6*, 57. [CrossRef]
19. Cha, J.W.; Kim, D.Y.; Jung, S.M. Distribution behavior of phosphorus and metallization of Iron Oxide in carbothermic reduction of high-phosphorus iron ore. *Metall. Mater. Trans. B* **2015**, *46*, 2165–2171. [CrossRef]
20. Han, H.L.; Duan, D.P.; Wang, X.; Chen, S. Innovative method for separating phosphorus and iron from high-phosphorus oolitic hematite by iron nugget process. *Metall. Mater. Trans. B* **2014**, *45*, 1634–1643. [CrossRef]
21. Chun, T.J.; Zhu, D.Q.; Pan, J.; He, Z. Preparation of alumina from iron powder from red mud by sodium salt roasting and magnetic separation. *Can. Metall. Q.* **2014**, *53*, 183–189. [CrossRef]